







## Article

# Electrochemically Deposited Zinc (Tetraamino)phthalocyanine as a Light-activated Antimicrobial Coating Effective against *S. aureus*

Ivan Gusev <sup>1,2</sup>, Marli Ferreira <sup>2</sup>, Davy-Louis Versace <sup>3,\*</sup>, Samir Abbad-Andaloussi <sup>4</sup>, Sandra Pluczyk-Małek <sup>1,2</sup>, Karol Erfurt <sup>1</sup>, Alicja Duda <sup>1</sup>, Przemysław Data <sup>2</sup> and Agata Blacha-Grzechnik <sup>1,2,\*</sup>

<sup>1</sup> Faculty of Chemistry, Silesian University of Technology, Strzody 9, 44-100 Gliwice, Poland; ivan.gusev@polsl.pl (I.G.); sandra.pluczyk-malek@polsl.pl (S.P.-M.); karol.erfurt@polsl.pl (K.E.); alicjaa.duda@gmail.com (A.D.)

<sup>2</sup> Centre for Organic and Nanohybrid Electronics, Silesian University of Technology, Konarskiego 22b, 44-100 Gliwice, Poland; marli.ferreira@polsl.pl (M.F.); przemyslaw.data@polsl.pl (P.D.)

<sup>3</sup> Institut de Chimie et des Matériaux Paris-Est (ICMPE, UMR-CNRS 7182-UPEC), 2-8 Rue Henri Dunant, 94320 Thiais, France

<sup>4</sup> Laboratoire Eau, Environnement, Systèmes Urbains (LEESU), UMR-MA 102, Université Paris-Est Créteil (UPEC), 61 Avenue Général de Gaulle, 94010 Créteil Cedex, France; abbad@u-pec.fr

\* Correspondence: davy-louis.versace@u-pec.fr (D.-L.V.); agata.blacha@polsl.pl (A.B.-G.)

**Abstract:** Light-activated antimicrobial coatings are currently considered to be a promising approach for the prevention of nosocomial infections. In this work, we present a straightforward strategy for the deposition of a photoactive biocidal organic layer of zinc (tetraamino)phthalocyanine (ZnPcNH<sub>2</sub>) in an electrochemical oxidative process. The chemical structure and morphology of the resulting layer are widely characterized by microscopic and spectroscopic techniques, while its ability to photogenerate reactive oxygen species (ROS) is investigated in situ by UV-Vis spectroscopy with  $\alpha$ -terpinene or 1,3-diphenylisobenzofuran as a chemical trap. It is shown that the ZnPcNH<sub>2</sub> photosensitizer retained its photoactivity after immobilization, and that the reported light-activated coating exhibits promising antimicrobial properties towards *Staphylococcus aureus* (*S. aureus*).

**Keywords:** electrochemical deposition; light-activated antimicrobial layer; reactive oxygen species (ROS); phthalocyanines; photosensitizers



**Citation:** Gusev, I.; Ferreira, M.; Versace, D.-L.; Abbad-Andaloussi, S.; Pluczyk-Małek, S.; Erfurt, K.; Duda, A.; Data, P.; Blacha-Grzechnik, A. Electrochemically Deposited Zinc (Tetraamino)phthalocyanine as a Light-activated Antimicrobial Coating Effective against *S. aureus*. *Materials* **2022**, *15*, 975. <https://doi.org/10.3390/ma15030975>

Academic Editor: Karla A. Batista

Received: 14 December 2021

Accepted: 23 January 2022

Published: 27 January 2022

**Publisher's Note:** MDPI stays neutral with regard to jurisdictional claims in published maps and institutional affiliations.



**Copyright:** © 2022 by the authors. Licensee MDPI, Basel, Switzerland. This article is an open access article distributed under the terms and conditions of the Creative Commons Attribution (CC BY) license (<https://creativecommons.org/licenses/by/4.0/>).

## 1. Introduction

In recent years, thin layers of organic and/or inorganic photosensitizers have gained wide research interest for application as antimicrobial coatings deposited on the surfaces of objects that are used daily. The main advantage of such structures is their remarkable biocidal efficiency against bacteria, viruses, and fungi. This makes them an attractive alternative to classical antimicrobial coatings containing poly(ethylene glycol) chains, silver or copper nanoparticles, quaternary ammonium salts or cations, fluorinated polymers, etc. [1,2]. The antimicrobial action of photoactive layers is based on the formation of so-called reactive oxygen species (ROS), including superoxides, peroxides, and singlet oxygen [3]. ROS act in a highly effective and non-selective manner (e.g. via the oxidation of enzymes, by increasing ions' permeability by the cell wall) against microorganisms, which, in turn, strongly reduces the possibility of the development of resistance by microbes [4–6]. Until now, light-activated antimicrobial coatings containing, e.g., phenothiazine, porphyrin, or fullerene photosensitizers have been successfully applied against *Staphylococcus aureus*, *Escherichia coli*, *Clostridium difficile*, *Candida albicans*, and *Pseudomonas aeruginosa* [7–14]. However, the practical usage of such photoactive layers is quite limited, and intense research is conducted in order to overcome key constraints, such as (photo)stability, long-term action, or the ease and accessibility of a deposition procedure.

For many years, phthalocyanines (Pcs) have been mainly investigated as promising candidates for application in (opto)electronics. Until recently, Pcs in a free-base form or with a central metal have been used in organic photovoltaic devices (OPVs) [15–17], organic light-emitting diodes (OLEDs) [18,19], or gas sensors [20–22]. Their effectiveness as photoinitiating systems [23,24] and photosensitizers [25,26] has also been reported. Moreover, it has been shown that the photosensitizing abilities of Pcs can be tuned by changing the central metal atom and/or by the introduction of outer functional groups.

Taking into account the above, in this work, we aimed to investigate the possibility of applying an electrodeposited Pc-based photoactive layer as a light-activated antimicrobial coating. Thus, zinc (tetraamino)phthalocyanine ( $\text{ZnPcNH}_2$ ) was selected as a primary photosensitizer molecule. The choice was first made based on the fact that Zn-containing Pcs show considerable efficiency of ROS production [27,28] and high antimicrobial properties [12,29]. Secondly, as shown in our previous work, the outer primary amino groups can be used in the electrochemically driven deposition of Pcs [30]. The presented novel, straightforward strategy, consisting of an electrochemical oxidation of primary amino groups present in the  $\text{ZnPcNH}_2$  structure, may be beneficial for the formation of a layer on conductive substrates. The deposited coating is widely characterized by means of spectroscopic and microscopic techniques. It is shown that the immobilized  $\text{ZnPcNH}_2$  photosensitizer is able to produce ROS under red laser or white light illumination and thus shows a light antimicrobial response against *Staphylococcus aureus* (*S. aureus*).

## 2. Materials and Methods

### 2.1. Materials

Zinc (tetraamino)phthalocyanine ( $\text{ZnPcNH}_2$ ) was synthesized based on previous works [31,32]. The synthesis procedure and the identification of the obtained product are described in the Supporting Information.

Dimethylformamide (DMF;  $\geq 99.8\%$ , Sigma Aldrich, St. Louis, MO, USA) containing tetrabutylammonium tetrafluoroborate ( $\text{TBABF}_4$ ; 99%, Sigma Aldrich, St. Louis, MO, USA) was used as an electrolyte solution for the electrochemical deposition of  $(\text{ZnPcNH}_2)_{\text{layer}}$ . Indium tin oxide/borosilicate glass (ITO) purchased from Präzisions Glas & Optik GmbH (PGO, Iserlohn, Germany) was used as a support. ROS photogeneration was investigated in  $\alpha$ -terpinene (TCI; purity > 90%)–acetonitrile (Sigma Aldrich, St. Louis, MO, USA) or 1,3-diphenylisobenzofuran (DPBF; Acros Organics, Geel, Belgium, purity > 97%)–methanol (Acros Organics, Geel, Belgium, 99.9%) systems.

### 2.2. Formation and Characterization of $(\text{ZnPcNH}_2)_{\text{layer}}$

$(\text{ZnPcNH}_2)_{\text{layer}}$  was formed on ITO or a platinum plate from 0.1 mM solution of  $\text{ZnPcNH}_2$  in 0.1 M  $\text{TBABF}_4$ /DMF. The starting solution was homogenized with an ultrasonic mixer and purged with argon for 15 minutes to remove oxygen. The process of electrochemical deposition was conducted using a cyclic voltammetry (CV) technique and a CHI 660C electrochemical workstation (CH Instruments Inc., Austin, TX, USA). A three-electrode setup was used: ITO or Pt as a working electrode, Ag wire as a pseudo-reference electrode, and glassy carbon (GC) as a counter electrode. The electrodes were copiously rinsed with DMF and mounted in a Teflon holder prior to use. The electrochemical deposition was conducted by means of cyclic voltammetry (CV) with the following process parameters: the potential range (−1.8; 1.4) V, 10 scan cycles, and a scan rate of 0.1 V/s. Ferrocene ( $\text{Fc}/\text{Fc}^+$ ) was used as a reference for the potential calibration.

The morphology of the layer was investigated using scanning electron microscopy (SEM) and atomic force microscopy (AFM). SEM images were acquired using Phenom ProX with an accelerating voltage equal to 15 kV and a magnification between 15,000 $\times$  and 20,000 $\times$ . The samples were sputter coated with 10 nm of gold film (Q150R Quorum Technologies, Laughton, East Sussex, UK) before SEM imaging. The images were analyzed with Phenom software. AFM investigations were conducted using Nanosurf CoreAFM working in a contact mode with the standard contact-mode AFM HQ:CSC17/Al BS (Mikro-

Masch, Tallinn, Estonia) probe (resonance frequency 13 kHz; force constant  $0.18 \text{ Nm}^{-1}$ ). The images were processed with the use of Gwyddion SPM (Brno University of Technology, Brno, Czech Republic).

UV–Vis spectra of the  $\text{ZnPcNH}_2$  solution in DMF and  $(\text{ZnPcNH}_2)_{\text{layer}}$  supported on ITO were acquired with a Hewlett Packard 8452A UV–Vis spectrometer. IR spectra of  $\text{ZnPcNH}_2$  powder and  $(\text{ZnPcNH}_2)_{\text{layer}}$  deposited on a platinum plate were recorded within the  $3500\text{--}700 \text{ cm}^{-1}$  range in attenuated total reflectance (ATR) mode using a Perkin Elmer Spectrum Two IR spectrometer (Hopkinton, MA, USA).

### 2.3. Reactive Oxygen Species (ROS) Photogeneration and Microbiological Analysis

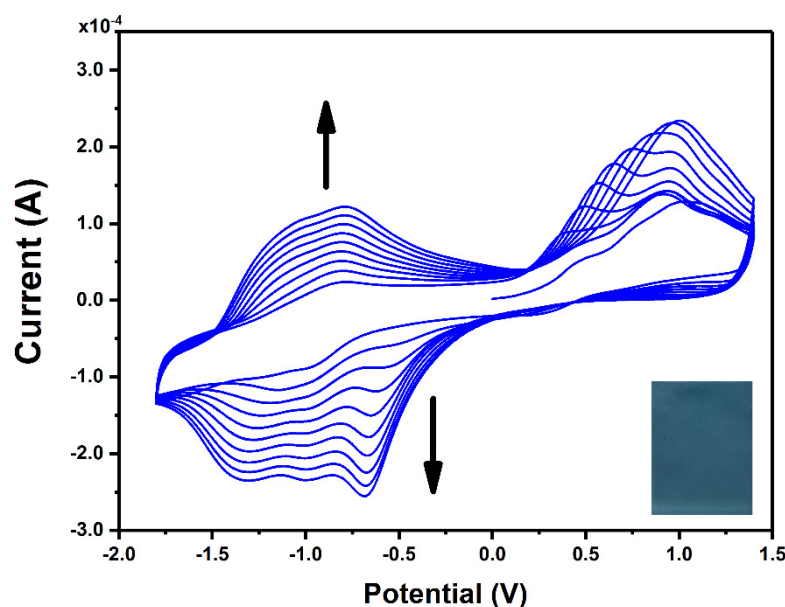
The process of ROS photogeneration was investigated either under 638 nm diode laser (Oxxius LBX-638-150-ELL-PP, Lannion, France, power reduced to 20 mW) or white light (Fiber-Coupled Xenon Light Source, Newton, NJ, USA, SLS205, 75 W, Thorlabs) illumination. In the first case, a DPBF trap was used with 0.05 mM solution in methanol, while in the second case, the trap was used with 0.05 mM solution of  $\alpha$ -terpinene in acetonitrile. The experimental setup was arranged in this way so that a photoactive layer supported on a glass plate was put in a quartz cuvette (Hellma Analytics, Müllheim, Germany,  $10 \times 4 \text{ mm}$ ). It was illuminated with a light source, while UV–Vis spectra of the chemical traps were collected in situ with a Hewlett Packard 8452A UV–Vis spectrometer (Palo Alto, CA, USA) along a direction perpendicular to the layer's illumination. The course of ROS production was observed by a drop of DPBF or  $\alpha$ -terpinene absorbance at 410 nm or 266 nm, respectively.

The antibacterial properties of the  $\text{ZnPcNH}_2$ -derived coatings, glass, and ITO surfaces were evaluated against *S. aureus* ATCC12000 according to previously described procedures [13,33,34]. The corresponding coatings were immersed in a bacterial solution for 24 h prior to visible-light activation, in order to maximize bacterial adhesion on surfaces. Then, half of the samples were kept in the dark while half of them were illuminated for 1 h on each side under a solar emission lamp. Following adhesion, all the defined square samples were rinsed seven times with sterile NaCl solution (0.9% *w/v*) to remove the non-adherent or dead bacteria from each surface. Then, samples were immersed in 3 mL of sterile saline solution and sonicated for 5 min in order to detach the viable bacteria from the surface of the studied samples. This solution was serially diluted by 10 to  $10^5$  factors. An amount of 100  $\mu\text{L}$  of each diluted and detached microorganism solution was then introduced on the surface of a Plat Count agar plate. This process was repeated as many times as there were dilutions. The total amount of viable bacteria was determined by counting the colony-forming units, after 48 h of incubation of the agar plates at  $37^\circ \text{C}$  (for each dilution), and levels of adhesion were given as numbers of counted bacteria/ $\text{cm}^2$  ( $\text{cm}^2$  corresponds to the surface of the defined samples). Four experiments were conducted on each sample.

## 3. Results and Discussion

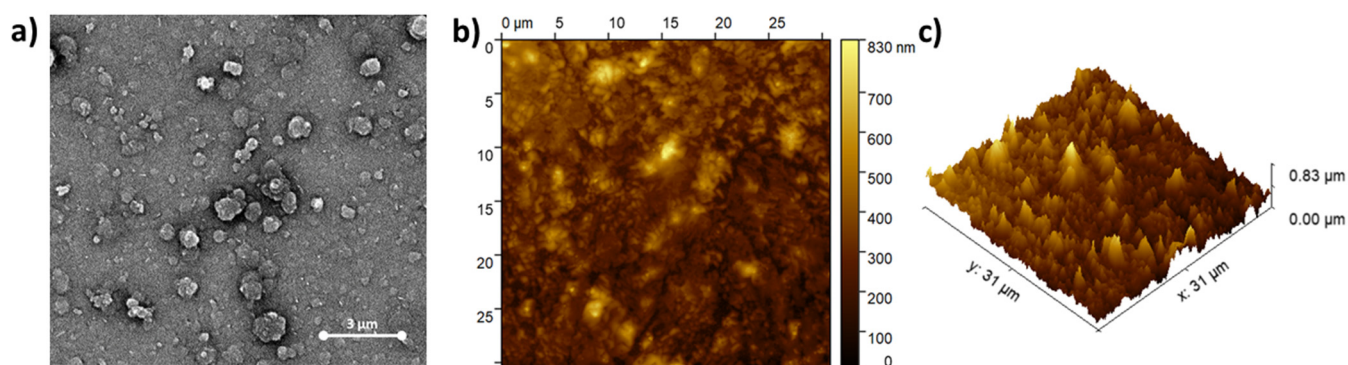
### 3.1. Formation and Spectroscopic and Microscopic Characterization of $(\text{ZnPcNH}_2)_{\text{layer}}$

Figure 1 presents CV curves recorded during continuous scanning in an electrolyte solution containing  $\text{ZnPcNH}_2$ . In the first anodic scan, an irreversible oxidation can be observed at ca. 0.75 V vs. Ag, which can be assigned to the oxidation of the primary amino group of  $\text{ZnPcNH}_2$  to a radical cation, similar to the electro-oxidation of the aniline monomer [35]. A steady increase in the registered current in the broad potential range during continuous scanning can be observed, confirming the formation of the electroactive layer on the surface of the ITO electrode. The newly occurring redox couples at ca.  $-0.75 \text{ V}$  and  $-1.25 \text{ V}$  arise from the electrochemical activity of the ZnPc layer [36–39]. In the course of the 10 scan cycles of the electrodeposition process, a uniform blue-green  $(\text{ZnPcNH}_2)_{\text{layer}}$  was synthesized on the ITO surface (Figure 1 inset).



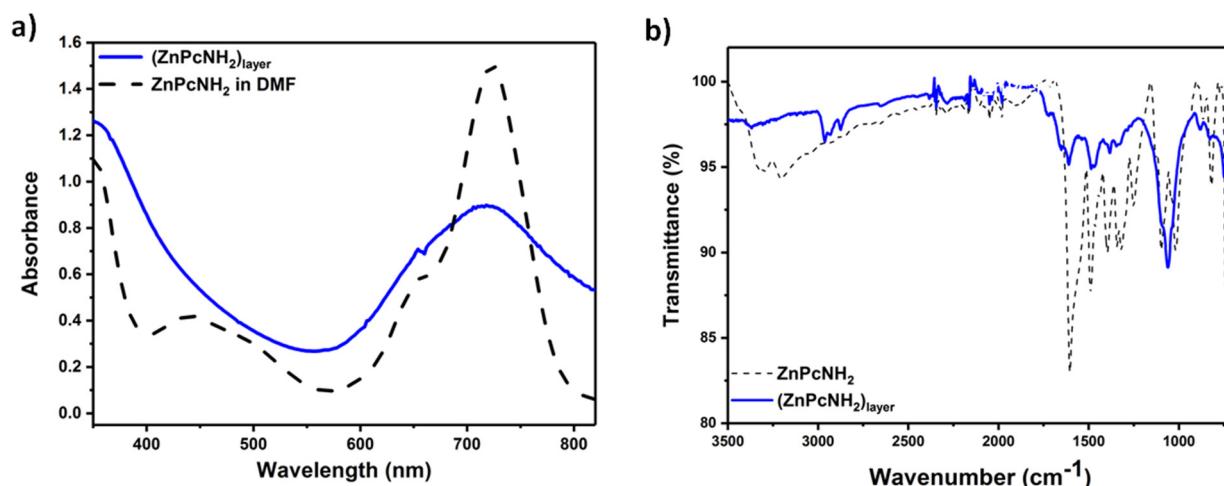
**Figure 1.** CV curves recorded for the ITO working electrode in 0.1 mM ZnPcNH<sub>2</sub> electrolyte solution (0.1 M TBABF<sub>4</sub>/DMF). Inset: photography of (ZnPcNH<sub>2</sub>)<sub>layer</sub> electrodeposited on ITO.

The morphology of (ZnPcNH<sub>2</sub>)<sub>layer</sub> on ITO was investigated using SEM and AFM techniques. An SEM image of ITO covered with ZnPcNH<sub>2</sub> is shown in Figure 2a. Spherical crystallites, typical for solution-deposited ZnPc films [40,41], sized within the 0.6–1.3 μm range, can be observed. Further, AFM studies confirmed the continuous coverage of the ITO surface, as shown in the exemplary AFM topography 31 × 31 μm<sup>2</sup> image shown in Figure 2b. An AFM image shown in Figure 2c also confirms the presence of rather vertically oriented crystallites. This is in contrast to ZnPc films deposited on a heated substrate with the PVD technique which have a rather ribbon-like structure [42]. The root mean square roughness (RMS) value for the presented area of the film was 100.9 nm.



**Figure 2.** (a) SEM and (b,c) AFM images of (ZnPcNH<sub>2</sub>)<sub>layer</sub> electrodeposited on ITO.

The optical properties and the chemical structure of (ZnPcNH<sub>2</sub>)<sub>layer</sub> were characterized by UV–Vis and IR spectroscopies, respectively. UV–Vis spectra of the solution of ZnPcNH<sub>2</sub> in DMF and (ZnPcNH<sub>2</sub>)<sub>layer</sub> deposited on ITO are presented in Figure 3a. The characteristic B (Soret band) and Q bands ( $\pi \rightarrow \pi^*$  transition band) for ZnPcNH<sub>2</sub>, both in a solution phase and in the form of a layer, can be observed at ca. 350 nm and 720 nm, respectively. The latter is significantly broadened in the case of the layer, possibly due to the aggregation of ZnPc molecules [36,43,44]. Notably, the deposited Pc layer exhibits strong and broad absorption in the visible range, which should be advantageous for a white light-driven photosensitization process.



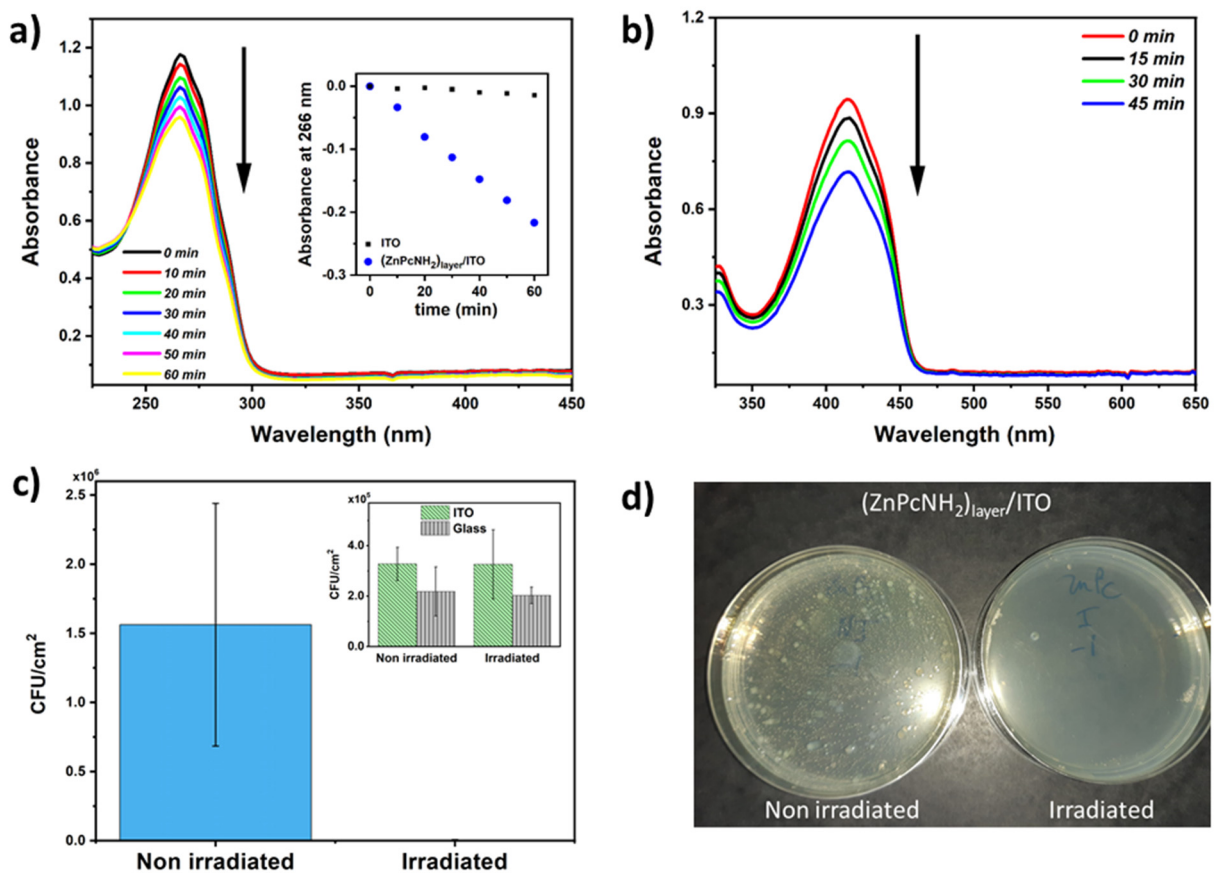
**Figure 3.** (a) UV–Vis of ZnPcNH<sub>2</sub> (black dashed line) and (ZnPcNH<sub>2</sub>)<sub>layer</sub> (blue line); (b) ATR-IR spectra of ZnPcNH<sub>2</sub> (black dashed line) and (ZnPcNH<sub>2</sub>)<sub>layer</sub> (blue line).

Figure 3b presents the ATR-IR spectra recorded for the ZnPcNH<sub>2</sub> powder and (ZnPcNH<sub>2</sub>)<sub>layer</sub> deposited on a Pt plate. Both spectra reveal the presence of the characteristic stretching vibrations of H-C bonds within Pc's ring at ca. 2950 cm<sup>-1</sup> [45]. Next, the C-N and C-C stretching vibrations in the isoindole part can be observed at 1260 ± 5 and 1327 ± 10 cm<sup>-1</sup>, respectively [45], while stretching vibrations of the Zn-N bond can be observed at 820 ± 6 cm<sup>-1</sup> [46], and out-of-plane bending of C-H bonds at 735 cm<sup>-1</sup> [47]. The presence of the metal-free Pc in the structure of the layer can be excluded based on the absence of N-H vibrations within the Pc ring that typically occur at ca. 1000 cm<sup>-1</sup> [47]. Finally, the clear difference between spectra of the monomer and the layer can be seen above 3000 cm<sup>-1</sup>, where the stretching vibrations of amino groups occur [48]. In the case of ZnPcNH<sub>2</sub>, two bands at 3203 and 3304 cm<sup>-1</sup> are present that are significantly less intense in the case of (ZnPcNH<sub>2</sub>)<sub>layer</sub>. This confirms that the primary amino groups are involved in the process of the layer's electrodeposition. The full assignment of the observed peaks is presented in Table S1.

### 3.2. Reactive Oxygen Species (ROS) Photogeneration and Antimicrobial Properties of (ZnPcNH<sub>2</sub>)<sub>layer</sub>

In the next step, the process of ROS photogeneration by the electrodeposited Pc layer was investigated under white light illumination, using indirect ROS detection employing UV–Vis spectroscopy to follow the changes in the concentration of α-terpinene, i.e., a chemical trap [49]. An exemplary UV–Vis spectra of α-terpinene in ACN recorded in the course of the illumination of (ZnPcNH<sub>2</sub>)<sub>layer</sub>/ITO are shown in Figure 4a. A successive decrease in the absorbance of α-terpinene at 266 nm can be observed, when (ZnPcNH<sub>2</sub>)<sub>layer</sub> is illuminated. Notably, the drop is significantly higher than in the case of uncovered ITO (Figure 4a, inset). This confirms that the chemical trap reacts with ROS produced by the Pcs-containing layer [50]. Importantly, since no new band arises in the UV–Vis spectra during the photoprocess, it can be stated that (ZnPcNH<sub>2</sub>)<sub>layer</sub> is stable and that the immobilized photosensitizers are not released into the environment.

Additionally, the photogeneration of ROS by (ZnPcNH<sub>2</sub>)<sub>layer</sub> was confirmed with a DPBF trap. In this case, a 638 nm diode laser was used as an illumination source because DPBF is not stable under white light [51]. As shown in Figure 4b, a clear drop in the absorbance at 410 nm can be observed, which is associated with a reaction of DPBF with the generated ROS. Similar to the acetonitrile solution, the photoactive layer remains stable in contact with methanol.



**Figure 4.** (a) UV–Vis spectra of  $\alpha$ -terpinene (ACN solution) recorded during illumination of  $(\text{ZnPcNH}_2)_{\text{layer}}$ ; inset: a drop in absorbance at 266 nm during illumination of unmodified ITO and  $(\text{ZnPcNH}_2)_{\text{layer}}/\text{ITO}$ . (b) UV–Vis spectra of DPBF (methanol solution) recorded during illumination of  $(\text{ZnPcNH}_2)_{\text{layer}}$ . (c) Evolution of colony-forming units, CFU/cm<sup>2</sup> (for *S. aureus*), at the surface of the non-irradiated and irradiated  $(\text{ZnPcNH}_2)_{\text{layer}}/\text{ITO}$ ; inset: ITO and glass,  $p < 0.001$ ,  $n = 4$ . (d) Optical images of *S. aureus* colonies on Petri dish after 48 h of incubation at 37 °C that adhered to the  $(\text{ZnPcNH}_2)_{\text{layer}}/\text{ITO}$  surface with and without irradiation.

The capability of the  $\text{ZnPcNH}_2$ -derived coating to inhibit *S. aureus* adhesion was assessed with and without visible-light illumination and compared with reference samples, i.e., ITO and glass surfaces (Figure 4c). Prior to anti-adhesion experiments, samples were incubated in a *S. aureus* solution for 24 h to allow optimal adhesion of *S. aureus* on coatings. Interestingly, when the incubated coatings were illuminated under visible light, a tremendous inhibition of the bacterial adhesion was observed on the  $\text{ZnPc}$ -containing coating: *S. aureus* inhibition under light reached up to 99.8% (Figure 4d). Importantly, visible light has no influence on the adhesion or proliferation of *S. aureus* on ITO and glass surfaces (Figure 4c, inset). These interesting results can be easily explained by the production of reactive oxygen species at the surface of the phthalocyanine-derived coatings under light activation, as previously described. These results point out the high potentiality of photoactivated coatings for disinfection applications.

#### 4. Conclusions

In this work,  $\text{ZnPcNH}_2$  photosensitizer was deposited on ITO/glass surface in a straightforward electrochemical process that involved an oxidation of the outer primary amino groups present in the Pc structure. The chemical structure of the formed layer was confirmed by ATR-IR spectroscopy. It was shown that  $(\text{ZnPcNH}_2)_{\text{layer}}$  possesses several advantages such as broadband absorption in the visible region and high environmental stability, even in organic solvents. The resulting coating can be activated by white light

illumination to effectively produce reactive oxygen species. This proves that immobilized ZnPcNH<sub>2</sub> retains its photosensitizing properties. Finally, it was shown that (ZnPcNH<sub>2</sub>)<sub>layer</sub> is active against *S. aureus*, there was a 99.8% light-associated decrease in the number of the adhered bacteria. To sum up, the presented results confirm that with a proper design of a photosensitizer molecule's structure, an efficient light-activated antimicrobial layer can be deposited in a simple electrodeposition process. In this work, ITO/glass or platinum was used as a support. However, it is believed that, since the deposition process is conducted in an oxygen-free organic environment under a rather low oxidative potential, it may be attractive for covering various (semi)conductive materials, irrespective of size or shape.

**Supplementary Materials:** The following are available online at <https://www.mdpi.com/article/10.3390/ma15030975/s1>: Synthesis and characterization of ZnPcNH<sub>2</sub> monomer, Table S1: Assignment of IR signals for ZnPcNH<sub>2</sub> monomer and (ZnPcNH<sub>2</sub>)<sub>layer</sub>.

**Author Contributions:** Conceptualization, A.B.-G.; methodology, M.F., D.-L.V. and A.B.-G.; validation, M.F., D.-L.V. and A.B.-G.; formal analysis, M.F., D.-L.V., S.P.-M. and A.B.-G.; investigation, I.G., M.F., D.-L.V., S.A.-A., S.P.-M., K.E., A.D. and A.B.-G.; writing—original draft preparation, M.F., D.-L.V. and A.B.-G.; writing—review and editing, A.B.-G.; visualization, M.F., D.-L.V., S.P.-M. and A.B.-G.; supervision, P.D. and A.B.-G.; project administration, P.D. and A.B.-G.; funding acquisition, I.G., P.D. and A.B.-G. All authors have read and agreed to the published version of the manuscript.

**Funding:** This work was financially supported by the First Team program of the Foundation for Polish Science co-financed by the European Union under the European Regional Development Fund (project number: First TEAM POIR.04.04.00-00-4668/17-00). I.G. and A.B.-G. kindly acknowledge the support received from the Polish Budget Funds for Scientific Research in 2021 as core funding for R&D activities in the Silesian University of Technology—funding for young researchers (grant numbers: 04/040/BKM21/0160 and 04/040/BKM21/0171, respectively). The authors are grateful to the training actions funded by the European Union's Horizon 2020 research and innovation program under grant agreement no. 952008.

**Institutional Review Board Statement:** Not applicable.

**Informed Consent Statement:** Not applicable.

**Data Availability Statement:** Data are presented in the article and Supplementary Materials.

**Conflicts of Interest:** The authors declare no conflict of interest.

## References

1. Sautrot-Ba, P.; Malval, J.-P.; Weiss-Maurin, M.; Paul, J.; Blacha-Grzechnik, A.; Tomane, S.; Mazeran, P.-E.; Lalevée, J.; Langlois, V.; Versace, D.-L. Paprika, Gallic Acid, and Visible Light: The Green Combination for the Synthesis of Biocide Coatings. *ACS Sustain. Chem. Eng.* **2018**, *6*, 104–109. [[CrossRef](#)]
2. Hwang, G.B.; Allan, E.; Parkin, I.P. White Light-Activated Antimicrobial Paint using Crystal Violet. *ACS Appl. Mater. Interfaces* **2015**, *8*, 15033–15039. [[CrossRef](#)] [[PubMed](#)]
3. Walker, T.; Canales, M.; Noimark, S.; Page, K.; Parkin, I.; Faull, J.; Bhatti, M.; Ciric, L. A Light-Activated Antimicrobial Surface Is Active Against Bacterial, Viral and Fungal Organisms. *Sci. Rep.* **2017**, *7*, 15298. [[CrossRef](#)] [[PubMed](#)]
4. Wainwright, M.; Crossley, K.B. Photosensitising agents—circumventing resistance and breaking down biofilms: A review. *Int. Biodeterior. Biodegrad.* **2004**, *53*, 119–126. [[CrossRef](#)]
5. Spagnul, C.; Turner, L.C.; Boyle, R.W. Immobilized photosensitizers for antimicrobial applications. *J. Photochem. Photobiol. B Biol.* **2015**, *150*, 11–30. [[CrossRef](#)]
6. Dahl, T.; RobertMiddenand, W.; Hartman, P. Pure singlet oxygen cytotoxicity for bacteria. *Photochem. Photobiol.* **1987**, *46*, 345–352. [[CrossRef](#)]
7. Peveler, W.J.; Noimark, S.; Al-Azawi, H.; Hwang, G.B.; Crick, C.R.; Allan, E.; Edel, J.B.; Ivanov, A.; MacRobert, A.J.; Parkin, I.P. Covalently Attached Antimicrobial Surfaces Using BODIPY: Improving Efficiency and Effectiveness. *ACS Appl. Mater. Interfaces* **2018**, *10*, 98–104. [[CrossRef](#)]
8. Piccirillo, C.; Perni, S.; Gil-Thomas, J.; Prokopovich, P.; Wilson, M.; Pratten, J.; Parkin, I.P. Antimicrobial activity of methylene blue and toluidine blue O covalently bound to a modified silicone polymer surface. *J. Mater. Chem.* **2009**, *19*, 6167–6171. [[CrossRef](#)]
9. Decraene, V.; Pratten, J.; Wilson, M. Novel Light-Activated Antimicrobial Coatings Are Effective Against Surface-Deposited *Staphylococcus aureus*. *Curr. Microbiol.* **2008**, *57*, 269–273. [[CrossRef](#)]

10. Ballatore, M.B.; Durantini, J.; Gsponer, N.S.; Suarez, M.B.; Gervaldo, M.; Otero, L.; Spesia, M.; Milanesio, M.E.; Durantini, E.N. Photodynamic Inactivation of Bacteria Using Novel Electrogenerated Porphyrin-Fullerene C60 Polymeric Films. *Environ. Sci. Technol.* **2015**, *49*, 7456–7463. [[CrossRef](#)]
11. Noimark, S.; Dunnill, C.; Parkin, I. Shining light on materials—A self-sterilising revolution. *Adv. Drug Deliv. Rev.* **2013**, *65*, 570–580. [[CrossRef](#)] [[PubMed](#)]
12. Grammatikova, N.E.; George, L.; Ahmed, Z.; Candeias, N.R.; Durandin, N.A.; Efimov, A. Zinc phthalocyanine activated by conventional indoor light makes a highly efficient antimicrobial material from regular cellulose. *J. Mater. Chem. B* **2019**, *7*, 4379–4384. [[CrossRef](#)]
13. Condat, M.; Mazeran, P.-E.; Malval, J.-P.; Lalevée, J.; Morlet-Savary, F.; Renard, E.; Langlois, V.; Andalloussi, S.A.; Versace, D.-L. Photoinduced curcumin derivative-coatings with antibacterial properties. *RSC Adv.* **2015**, *5*, 85214–85224. [[CrossRef](#)]
14. Sautrot-Ba, P.; Jockusch, S.; Nguyen, T.-T.-T.; Grande, D.; Chiapionne, A.; Abbad-Andaloussi, S.; Pan, M.; Méallet-Renault, R.; Versace, D.-L. Photoinduced synthesis of antibacterial hydrogel from aqueous photoinitiating system. *Eur. Polym. J.* **2020**, *138*, 109936. [[CrossRef](#)]
15. Urbani, M.; Ragoussi, M.-E.; Nazeeruddin, M.K.; Torres, T. Phthalocyanines for dye-sensitized solar cells. *Co-Ord. Chem. Rev.* **2019**, *381*, 1–64. [[CrossRef](#)]
16. Tunç, G.; Güzel, E.; Şişman, I.; Ahsen, V.; Cárdenas-Jirón, G.; Gürek, A.G. Effect of new asymmetrical Zn(II) phthalocyanines on the photovoltaic performance of a dye-sensitized solar cell. *New J. Chem.* **2019**, *43*, 14390–14401. [[CrossRef](#)]
17. Suzuki, A.; Okumura, H.; Yamasaki, Y.; Oku, T. Fabrication and characterization of perovskite type solar cells using phthalocyanine complexes. *Appl. Surf. Sci.* **2019**, *488*, 586–592. [[CrossRef](#)]
18. Hamui, L.; Sánchez-Vergara, M.E.; Díaz-Ortega, N.; Salcedo, R. Comparative Study of Conduction Mechanisms in Disodium Phthalocyanine-Based Organic Diodes for Flexible Electronics. *Molecules* **2020**, *25*, 3687. [[CrossRef](#)]
19. Rai, V.; Gerhard, L.; Sun, Q.; Holzer, C.; Repän, T.; Krstić, M.; Yang, L.; Wegener, M.; Rockstuhl, C.; Wulfhekel, W. Boosting Light Emission from Single Hydrogen Phthalocyanine Molecules by Charging. *Nano Lett.* **2020**, *20*, 7600–7605. [[CrossRef](#)]
20. Bohrer, F.I.; Colesniuc, C.N.; Park, J.; Ruidiaz, M.E.; Schuller, I.K.; Kummel, A.C.; Trogler, W.C. Comparative Gas Sensing in Cobalt, Nickel, Copper, Zinc, and Metal-Free Phthalocyanine Chemiresistors. *J. Am. Chem. Soc.* **2008**, *131*, 478–485. [[CrossRef](#)]
21. Demir, F.; Yenilmez, H.Y.; Koca, A.; Bayır, Z.A. Metallo-phthalocyanines containing thiazole moieties: Synthesis, characterization, electrochemical and spectroelectrochemical properties and sensor applications. *J. Electroanal. Chem.* **2019**, *832*, 254–265. [[CrossRef](#)]
22. Kaya, E.N.; Şenocak, A.; Klyamer, D.D.; Demirbaş, E.; Basova, T.V.; Durmuş, M. Ammonia sensing performance of thin films of cobalt(II) phthalocyanine bearing fluorinated substituents. *J. Mater. Sci. Mater. Electron.* **2019**, *30*, 7543–7551. [[CrossRef](#)]
23. Breloy, L.; Brezová, V.; Blacha-Grzechnik, A.; Pisset, M.; Yildirim, M.S.; Yilmaz, I.; Yagci, Y.; Versace, D.-L. Visible Light Anthraquinone Functional Phthalocyanine Photoinitiator for Free-Radical and Cationic Polymerizations. *Macromolecules* **2020**, *53*, 112–124. [[CrossRef](#)]
24. Breloy, L.; Alcay, Y.; Yilmaz, I.; Breza, M.; Bourgon, J.; Brezová, V.; Yagci, Y.; Versace, D.-L. Dimethyl amino phenyl substituted silver phthalocyanine as a UV- and visible-light absorbing photoinitiator: In situ preparation of silver/polymer nanocomposites. *Polym. Chem.* **2021**, *12*, 1273–1285. [[CrossRef](#)]
25. Ishii, K. Functional singlet oxygen generators based on phthalocyanines. *Coord. Chem. Rev.* **2012**, *256*, 1556–1568. [[CrossRef](#)]
26. Ogunbayo, T.B.; Nyokong, T. Photophysical and photochemical properties of Ni(II), Pd(II) and Pt(II) aryloxo and alkylthio derivatised phthalocyanine. *J. Mol. Struct.* **2010**, *973*, 96–103. [[CrossRef](#)]
27. Ke, M.-R.; Eastel, J.M.; Ngai, K.L.K.; Cheung, Y.-Y.; Chan, P.K.S.; Hui, M.; Ng, D.K.P.; Lo, P.-C. Oligolysine-Conjugated Zinc(II) Phthalocyanines as Efficient Photosensitizers for Antimicrobial Photodynamic Therapy. *Chem.-Asian J.* **2014**, *9*, 1868–1875. [[CrossRef](#)]
28. Wan, Y.; Liang, Q.; Cong, T.; Wang, X.; Tao, Y.; Sun, M.; Li, Z.; Xu, S. Novel catalyst of zinc tetraamino-phthalocyanine supported by multi-walled carbon nanotubes with enhanced visible-light photocatalytic activity. *RSC Adv.* **2015**, *5*, 66286–66293. [[CrossRef](#)]
29. Mapukata, S.; Sen, P.; Osifeko, O.L.; Nyokong, T. The antibacterial and antifungal properties of neutral, octacationic and hexadecacationic Zn phthalocyanines when conjugated to silver nanoparticles. *Photodiagnosis Photodyn. Ther.* **2021**, *35*, 102361. [[CrossRef](#)]
30. Krzywiecki, M.; Pluczyk-Małek, S.; Powroźnik, P.; Ślusarczyk, C.; Król-Molenda, W.; Smykała, S.; Kurek, J.; Koptoń, P.; Łapkowski, M.; Blacha-Grzechnik, A. Chemical and Electronic Structure Characterization of Electrochemically Deposited Nickel Tetraamino-phthalocyanine: A Step toward More Efficient Deposition Techniques for Organic Electronics Application. *J. Phys. Chem. C* **2021**, *125*, 13542–13550. [[CrossRef](#)]
31. Jia, H.; Yao, Y.; Zhao, J.; Gao, Y.; Luo, Z.; Du, P. A novel two-dimensional nickel phthalocyanine-based metal-organic framework for highly efficient water oxidation catalysis. *J. Mater. Chem. A* **2018**, *6*, 1188–1195. [[CrossRef](#)]
32. Yüksel, F.; Gürek, A.G.; Lebrun, C.; Ahsen, V. Synthesis and solvent effects on the spectroscopic properties of octatosylamido phthalocyanines. *New J. Chem.* **2005**, *29*, 726–732. [[CrossRef](#)]
33. Sautrot-Ba, P.; Jockusch, S.; Malval, J.-P.; Brezová, V.; Rivard, M.; Abbad-Andaloussi, S.; Blacha-Grzechnik, A.; Versace, D.-L. Quinizarin Derivatives as Photoinitiators for Free-Radical and Cationic Photopolymerizations in the Visible Spectral Range. *Macromolecules* **2020**, *53*, 1129–1141. [[CrossRef](#)]



34. Condat, M.; Babinot, J.; Tomane, S.; Malval, J.-P.; Kang, I.-K.; Spillebout, F.; Mazeran, P.-E.; Lalevée, J.; Andalloussi, S.A.; Versace, D.-L. Development of photoactivable glycerol-based coatings containing quercetin for antibacterial applications. *RSC Adv.* **2016**, *6*, 18235–18245. [[CrossRef](#)]
35. Lokesh, K.S.; Adriaens, A. Electropolymerization of palladium tetraaminephthalocyanine: Characterization and supercapacitance behavior. *Dye. Pigment.* **2015**, *112*, 192–200. [[CrossRef](#)]
36. Koca, A.; Özkaya, A.R.; Selçukoğlu, M.; Hamuryudan, E. Electrochemical and spectroelectrochemical characterization of the phthalocyanines with pentafluorobenzyloxy substituents. *Electrochim. Acta* **2007**, *52*, 2683–2690. [[CrossRef](#)]
37. Kalkan, A.; Koca, A.; Bayır, Z.A. Unsymmetrical phthalocyanines with alkynyl substituents. *Polyhedron* **2004**, *23*, 3155–3162. [[CrossRef](#)]
38. Demirbaş, Ü.; Kobak, R.Z.U.; AKÇAY, H.T.; Ünlüer, D.; Koca, A.; Çelik, F.; Kantekin, H. Synthesis, characterization, electrochemical and spectroelectrochemical properties of novel peripherally tetra-1,2,4-triazole substituted phthalocyanines. *Synth. Met.* **2016**, *215*, 68–76. [[CrossRef](#)]
39. Manivannan, V.; Nevin, W.A.; Leznoff, C.C.; Lever, A.B.P. Electrochemistry and Spectroelectrochemistry of Polynuclear Zinc Phthalocyanines: Formation of Mixed Valence Cation Radical Species. *J. Coord. Chem.* **1988**, *19*, 139–158. [[CrossRef](#)]
40. Roy, D.; Das, N.M.; Shakti, N.; Gupta, P.S. Comparative study of optical, structural and electrical properties of zinc phthalocyanine Langmuir–Blodgett thin film on annealing. *RSC Adv.* **2014**, *4*, 42514–42522. [[CrossRef](#)]
41. Zhai, Z.; Xu, M. All-solution-processed small-molecule solar cells by stripping-transfer method. *J. Mater. Sci. Mater. Electron.* **2020**, *31*, 5789–5793. [[CrossRef](#)]
42. Cranston, R.R.; Lessard, B.H. Metal phthalocyanines: Thin-film formation, microstructure, and physical properties. *RSC Adv.* **2021**, *11*, 21716–21737. [[CrossRef](#)]
43. Topal, S.Z.; Işci, Ü.; Kumru, U.; Atilla, D.; Gürek, A.G.; Hirel, C.; Durmuş, M.; Tommasino, J.-B.; Luneau, D.; Berber, S.; et al. Modulation of the electronic and spectroscopic properties of Zn(ii) phthalocyanines by their substitution pattern. *Dalton Trans.* **2014**, *43*, 6897–6908. [[CrossRef](#)] [[PubMed](#)]
44. Socol, M.; Preda, N.; Costas, A.; Breazu, C.; Stanculescu, A.; Rasoga, O.; Popescu-Pelin, G.; Mihailescu, A.; Socol, G. Hybrid organic-inorganic thin films based on zinc phthalocyanine and zinc oxide deposited by MAPLE. *Appl. Surf. Sci.* **2020**, *503*, 144317. [[CrossRef](#)]
45. Seoudi, R.; El-Bahy, G.; El Sayed, Z. FTIR, TGA and DC electrical conductivity studies of phthalocyanine and its complexes. *J. Mol. Struct.* **2005**, *753*, 119–126. [[CrossRef](#)]
46. Saini, G.S.S.; Singh, S.; Kaur, S.; Kumar, R.; Sathe, V.; Tripathi, S.K. Zinc phthalocyanine thin film and chemical analyte interaction studies by density functional theory and vibrational techniques. *J. Phys. Condens. Matter* **2009**, *21*, 225006. [[CrossRef](#)]
47. Verma, D.; Dash, R.; Katti, K.S.; Schulz, D.L.; Caruso, A.N. Role of coordinated metal ions on the orientation of phthalocyanine based coatings. *Spectrochim. Acta Part A Mol. Biomol. Spectrosc.* **2008**, *70*, 1180–1186. [[CrossRef](#)]
48. Lee, J.U.; Kim, Y.D.; Jo, J.W.; Kim, J.P.; Jo, W.H. Efficiency enhancement of P3HT/PCBM bulk heterojunction solar cells by attaching zinc phthalocyanine to the chain-end of P3HT. *J. Mater. Chem.* **2011**, *21*, 17209–17218. [[CrossRef](#)]
49. Nyga, A.; Motyka, R.; Bussetti, G.; Calloni, A.; Jagadeesh, M.S.; Fijak, S.; Pluczyk-Malek, S.; Data, P.; Blacha-Grzechnik, A. Electrochemically deposited poly(selenophene)-fullerene photoactive layer: Tuning of the spectroscopic properties towards visible light-driven generation of singlet oxygen. *Appl. Surf. Sci.* **2020**, *525*, 146594. [[CrossRef](#)]
50. Ronzani, F.; Costarramone, N.; Blanc, S.; Benabbou, A.K.; LE Behec, M.; Pigot, T.; Oelgemöller, M.; Lacombe, S. Visible-light photosensitized oxidation of  $\alpha$ -terpinene using novel silica-supported sensitizers: Photooxygenation vs. photodehydrogenation. *J. Catal.* **2013**, *303*, 164–174. [[CrossRef](#)]
51. Entradas, T.; Waldron, S.; Volk, M. The detection sensitivity of commonly used singlet oxygen probes in aqueous environments. *J. Photochem. Photobiol. B Biol.* **2020**, *204*, 111787. [[CrossRef](#)] [[PubMed](#)]